PTEN regulates adipocyte progenitor growth, differentiation and cellular aging

Anna S. Kirstein[1], Stephanie Kehr[2], Michèle Nebe[1], Judith Lorenz[1], Melanie Penke[1], Jana Breitfeld[3], Diana Le Duc[4,5], Peter Kovacs[3], Peter F. Stadler[2,6], Wieland Kiess[1], Antje Garten[1]

[1] University Hospital for Children & Adolescents, Center for Pediatric Research, Leipzig University, Leipzig, Germany
[2] Bioinformatics Group, Department of Computer Science and Interdisciplinary Center for Bioinformatics, Leipzig University, Leipzig, Germany
[3] Medical Department III-Endocrinology, Nephrology, Rheumatology, Leipzig University Medical Center, Leipzig, Germany
[4] Institute of Human Genetics, Leipzig University Medical Center, Leipzig, Germany
[5] Department of Evolutionary Genetics, Max Planck Institute for Evolutionary Anthropology, Leipzig, Germany
[6] Max Planck Institute for Mathematics in the Sciences, Leipzig, Germany

Address of correspondence: Anna S. Kirstein

Leipzig University

Hospital for Children and Adolescents

Center for Pediatric Research Leipzig

Liebigstraße 21

04103 Leipzig

Germany

Anna.Kirstein@medizin.uni-leipzig.de

Running title: PTEN in adipocyte progenitor differentiation and aging

Keywords: PTEN Hamartoma Tumor Syndrome, Adipogenesis, Adipocyte, Lipoma, Cellular Senescence, Mesenchymal Stem Cells

Abstract

Adipose tissue distribution and insulin sensitivity are altered during aging. The tumor suppressor phosphatase and tensin homolog (PTEN) is known to negatively regulate the insulin signaling pathway and mutations influence adipose tissue redistribution. Germline *PTEN* pathogenic variants cause PTEN Hamartoma Tumor Syndrome (PHTS), which is associated with lipoma development in children. It remains unclear which mechanisms trigger this aberrant adipose tissue growth. Fat cell (adipocyte) progenitors lose their capacity to differentiate into adipocytes during continuous culture, while adipocyte progenitor cells (APCs) from PHTS patients' lipomas retain their adipogenic potential over a prolonged period. To investigate the role of PTEN in adipose tissue development we performed functional assays and RNA-sequencing of control and PTEN knockdown APCs. We assessed phenotypical differences as well as genes and pathways regulated in conditions of PTEN insufficiency. Reduction of PTEN levels using siRNA or CRISPR lead to an enhanced proliferation and differentiation of APCs. We observed that PTEN levels were upregulated during long term culture of wild type APCs. PTEN CRISPR cells showed less senescence after continuous culture compared to controls and the senescence marker *CDKN1A* (p21) was downregulated on protein and RNA level in PTEN knockdown cells. Cellular senescence was the most significantly enriched pathway found in gene set enrichment analysis of RNA from PTEN knockdown *vs*. control cells. These results provide evidence that PTEN is involved in the regulation of APCs proliferation, differentiation and senescence, thereby contributing to aberrant adipose tissue growth in PHTS patients.

Introduction

Adipose tissue distribution is altered during aging – while subcutaneous fat depots decrease in advanced age, fat accumulates in muscle, liver and bone marrow, leading to metabolic dysregulation (1). Responsiveness to insulin declines in adipocytes from older individuals and metabolic features related to fatty acid metabolism change (2, 3). Human adipose tissue contains mesenchymal stem cells (MSCs), which serve as adipocyte progenitors and contribute to adipose tissue regeneration throughout life (4). These cells are found within the stromal vascular fraction (SVF) of adipose tissue. Adipogenesis can be induced by insulin and other soluble factors *in vitro* (5). SVF cells from older individuals have a lower capacity for adipocyte differentiation (6) and during long term SVF cell culture the adipogenic potential declines (7). Inhibiting the phosphoinositide 3-kinase (PI3K)/AKT pathway in adipose progenitors using the mammalian target of rapamycin (mTOR) inhibitor rapamycin (8) or the PI3K inhibitor alpelisib (9) was shown to repress adipogenesis. Several studies link insulin signaling and aging. Mice with adipose tissue specific insulin receptor knockout had an increased lifespan (10), but the underlying mechanisms are controversial (11). Adipose tissue in these mice maintains mitochondrial activity and insulin-sensitivity during aging, indicating that insulin-sensitivity dynamics rather than insulin-resistance correlate with longevity (11, 12).

We observed that lipoma cells from a patient with *phosphatase and tensin homolog* (*PTEN*) germline pathogenic variant retain their differentiation capacity over a prolonged period (13). PTEN is a lipid and protein phosphatase, mainly catalyzing the dephosphorylation of the second messenger phosphatidylinositol-3,4,5-trisphosphate, resulting in a deactivation of the PI3K/AKT pathway signaling. PTEN is an important antagonist of this pathway, which is activated by a multitude of extracellular signals including insulin and insulin-like growth factor 1 (IGF-1). PI3K/AKT signaling generally promotes cellular growth and survival. The downstream target and central signaling molecule mTOR is a major regulator of protein and lipid synthesis, cell growth, proliferation, autophagy and metabolism (14). Loss of the tumor suppressor *PTEN* is common in cancer. *PTEN* haploinsufficiency caused by germline pathogenic variants leads to the rare genetic disease PTEN hamartoma tumor syndrome (PHTS). PHTS patients show a wide variety of phenotypes including hamartomas of the skin, breast and thyroid, intestinal polyps, macrocephaly, vascular malformations and lipoma formation (15). Widespread lipomatosis and lack of subcutaneous adipose tissue was observed in a boy with PHTS (16). It remains unclear which specific factors cause this localized adipose tissue overgrowth in PHTS patients.

Several mouse models with *PTEN* downregulation in adipose tissue (17, 18), adipose progenitor subpopulations (17, 18) or osteoblast progenitors (19, 20) display adipose

tissue redistribution and/or lipoma formation and partly recapitulate the human phenotype of PHTS. Overexpression of AKT in zebrafish also leads to lipoma formation, linking PI3K signaling to adipose tissue overgrowth (21). A high PTEN expression in adipose tissue (22) points to its importance in regulating normal adipose tissue function. *PTEN* pathogenic variants were found to lead to adipose tissue redistribution in mice (17, 18), with similar phenotypes also observed in humans (16).

To investigate the effects of PTEN downregulation in human adipose progenitor cells and create an *in vitro* model for PTEN insufficiency as seen in PHTS, we used SVF cells isolated from visceral adipose tissue of healthy donors and downregulated PTEN via siRNA or clustered regularly interspaced short palindromic repeats (CRISPR) system. We thereby observed phenomena associated with proliferation, differentiation and aging of fat cell progenitors pointing to a role for PTEN in lipoma formation.

Results

2.1 PTEN downregulation enhanced PI3K signaling and SVF cell proliferation

To examine the impact of PTEN loss on adipocyte development we performed siRNA mediated knockdown of PTEN (PTEN KD) in SVF cells from visceral adipose tissue of donors without *PTEN* mutation. As determined via Western blot analysis PTEN was reduced in the siRNA knockdown cells to 0.49 ± 0.04 fold ($p<0.0001$, Figure 1a). On mRNA level we found a reduction of *PTEN* expression to 0.33 ± 0.08 fold ($p<0.0001$, Figure 1b). The knockdown was stable during 7 days of proliferation (Figure S1A) and 8 days of differentiation (Figure S1B). To test the functional significance of the knockdown we investigated activation of downstream PI3K/AKT pathway components via phosphorylation. Phosphorylated AKT (pAKT (T308)) was elevated 22 ± 14 fold ($p=0.029$) and ribosomal protein S6 phosphorylation (pS6 (Ser235/236)) was increased 13.0 ± 5.5 fold ($p = 0.0008$) (Figure 1a).

siRNA mediated knockdowns are of transient nature, which is why we additionally performed *PTEN* knockouts using the CRISPR system in SVF cells (PTEN CR). On average, PTEN protein levels were reduced to 0.7 ± 0.3 fold ($p=0.27$), while pAKT (T308) was increased 8 ± 6 fold ($p = 0.24$) and pS6 (Ser235/236) was increased 14 ± 10 fold ($p=0.09$) (Figure 1c). *PTEN* mRNA was reduced to 0.56 ± 0.05 fold ($p = 0.0002$) in PTEN CR cells (Figure 1d). Using both methods, we achieved a similar reduction in PTEN levels, as seen in cells of a patient with germline heterozygous *PTEN* deletion (13).

We observed an enhanced proliferation in PTEN insufficient SVF cells. PTEN downregulation led to faster expansion to a similar extent in PTEN KD cells (1.4 ± 0.2 fold, $p=0.038$, Figure 2a) and in PTEN CR cells (1.5 ± 0.1 fold, $p=0.039$, Figure 2b). The higher

cell count was also reflected in a 1.09 ± 0.01 fold (p = 0.0043) higher fraction of proliferation marker Ki-67 positive cells as shown by immunofluorescence staining (Figure 2c).

2.2 PTEN downregulation restored adipogenic potential in high-passage SVF cells

SVF cells lose their capacity for adipocyte differentiation when cultured for several passages (7). In view of the high adipogenic potential observed in PTEN haploinsufficient lipoma cells, we asked whether PTEN downregulation could reverse this process. High-passage SVF cells (> 15 days in culture) which lost their adipocyte differentiation capacity, were transfected with *PTEN* or control siRNA and kept in adipogenic medium for 8 days. Nile Red lipid staining showed a 1.77 ± 0.07 fold (p = 0.0026) increase in differentiated cells after PTEN knockdown (Figure 3a). This finding was also supported by an increase in size of 3D spheroids of PTEN KD SVF cells in adipogenic medium (Figure 3b). While the size of control siRNA spheroids remained constant over 12 days, the size of PTEN KD spheroids was increased 1.23 ± 0.03 fold (p < 0.001). It was previously shown that the size of the spheroids corresponds to the degree of differentiation (13, 23).

Taking advantage of the stable PTEN downregulation, we observed differentiation capacity of PTEN CR cells 2–6 weeks after transfection. After long term culture only 5 ± 2 % of control cells differentiated into adipocytes during 8 days in adipogenic medium, while 24 ± 1 % of PTEN CR cells differentiated (Figure 3c). This is a 5.6 ± 1.9 fold (p=0.004) increase in differentiation in the CRISPR PTEN knockout cells. Expression of the adipocyte markers *adiponectin* (2.6 ± 0.6 fold, p=0.016), *fatty acid synthase* (*FASN*) (2.1 ± 0.8 fold, p=0.075) and *fatty acid binding protein 4* (*FABP4*) (1.9 ± 0.6 fold, p=0.078) was increased in PTEN CR cells compared to controls after 8 days in adipogenic medium, confirming these findings (Figure 3d).

2.3 PTEN levels were upregulated during cellular aging

Following the indication of restored differentiation capacity in aged SVF cells after PTEN downregulation, we wanted to check whether PTEN levels were regulated during long term culture of SVF cells. We analyzed levels of PTEN protein and AKT phosphorylation (pAkt) in primary SVF cells at different passages. In addition, we detected levels of the nicotinamide adenine dinucleotide (NAD) biosynthesis enzyme nicotinamide phosphoribosyltransferase (NAMPT) which is known to be downregulated during aging (24). PTEN levels rose during long term culture, while the ratio of pAKT (T308) to total AKT levels declined. A decline was also observed in the levels of NAMPT during long term culture (Figure 4a). We observed a reversion in PTEN KD cells, with NAMPT protein 1.6 ± 0.2 fold (p=0.0029) elevated in PTEN KD cells, while levels of the senescence

associated cell cycle regulator p21 protein were reduced to 0.33 ± 0.07 fold (p=0.0004) after PTEN KD (Figure 4b). We also found a reduction of *CDKN1A* (*p21*) (to 0.6 ± 0.06 fold, p=0.031) and senescence marker *CDKN2A* (*p16*) (to 0.68 ± 0.05 fold, p=0.014) mRNA in PTEN KD SVF cells (Figure S1C). After long term culture there were 1.58 ± 0.12 fold (p=0.0098) more senescence-associated β-galactosidase (SA-β-gal) positive cells found in the controls compared to PTEN CR cells, supporting a rejuvenating effect of PTEN downregulation (Figure 4c).

2.4 Expression changes after PTEN downregulation

We performed RNA-sequencing of PTEN KD and control SVF cells as an untargeted approach to identify genes and pathways regulated in conditions of PTEN downregulation (Supplement Tables S1 and S2 available at www.bioinf.uni-leipzig.de/publications/supplements/20-008). We found 1379 differentially expressed genes (adjusted p-value < 0.01), of which 170 had a log2 fold change (log2FC) >1 or <-1 (Figure 5a). More genes were upregulated 60% (829/1379) or 68% (115 of 170) than downregulated, corresponding to the pathway deactivating nature of PTEN (Figure 5b). Among the 50 most significantly differentially expressed genes only two were downregulated in PTEN KD (Figure 5b). Gene set enrichment analysis using StringDb (25) identified 18 significantly enriched Kyoto Encyclopedia of Genes and Genomes (KEGG) pathways (p < 0.05) (Figure 5c). The pathway most significantly enriched in PTEN KD compared to control SVF cells was *Cellular Senescence* (hsa04218) with altered gene expression levels for 28 out of 156 genes (p = 0.00056). Detailed networks of the regulated and other KEGG pathways relevant in the context of metabolism, aging and adipocyte progenitor cells can be found at the supporting information website: www.bioinf.uni-leipzig.de/publications/supplements/20-008 .

To identify genes relevant for lipoma development, adipose tissue function and adipogenesis we compared our gene set with two other gene sets; first a study by Le Duc *et al*. (26) comparing lipomas and subcutaneous adipose tissue of the same patient and second a study by Breitfeld *et al*. (27) comparing adipogenesis in inguinal and epididymal fat depots. We found an overlap of 36 genes (Supplementary Table S3), including some known regulators of adipogenesis like *FOXO1* (Nakae et al., 2003) and genes such as *RNF144B* which has no known function in adipose tissue yet. For validation we picked these two genes and analyzed their expression changes during 12 days of adipogenesis in a PHTS patients lipoma cells (LipPD1). We found *FOXO1* upregulated and *RNF144B* downregulated during adipocyte development (p < 0.001) (Supplementary Figure 1D).

Discussion

As a well-established tumor suppressor, PTEN is known for its anti-proliferative effects in many cell types. However, not much is known about the role of PTEN in adipocyte progenitors. Both obesity and lipoma formation are characterized by adipose tissue overgrowth. While it is known that in obesity both hypertrophy and hyperplasia contribute to adipose tissue expansion (28), it remains unclear whether these mechanisms also promote lipoma formation. Within this study, we investigated the mechanisms leading to aberrant adipose tissue growth and lipoma formation in patients with heterozygous *PTEN* mutations. A PTEN downregulation in adipocyte progenitor cells of approximately 50 % as observed in lipoma cells of a PHTS patient (13), lead to a several-fold activation of the PI3K downstream targets AKT and ribosomal protein S6. The overactivation of the PI3K pathway enhanced the proliferation of these cells, which is in line with the general cell cycle activating function of the pathway (29). We conclude that PTEN controls adipose tissue growth and inhibits adipocyte progenitor expansion under normal conditions. Conversely, reduction in the phosphatase PTEN may lead to adipose tissue hyperplasia and lipoma formation.

We previously observed that SVF cells obtained from a pediatric PHTS patients' lipoma retain their ability to differentiate into adipocytes over a prolonged period, while primary SVF cells from healthy donors lose their differentiation capacity after several passages (13). To investigate whether this effect is caused by a reduction in PTEN protein levels, we analyzed differentiation of SVF cells with and without PTEN knockdown. SVF cells that had already lost their capacity to differentiate into adipocytes differentiated again in 2D and 3D culture after siRNA mediated PTEN knockdown. SVF cells with stable CRISPR mediated PTEN downregulation kept their ability to undergo differentiation after long term culture. In support of the hypothesis that PTEN plays a role in regulating adipogenesis we identified several genes differentially expressed comparing PTEN KD and control cells. We validated two of these, *FOXO1* and *RNF144B*, analyzing their regulation during adipocyte differentiation. Since adipogenesis can be induced through insulin (5), the stimulating effects of PTEN downregulation on adipogenesis might be mediated through a higher insulin sensitivity. It is known that reduction in PTEN leads to higher insulin sensitivity while body weight increases (30), which could account for these effects. The adipogenic potential of SVF cells from older animals is decreased (4). These age related effects could be coupled to insulin sensitivity, which is known to decrease as well with old age (1).

Interestingly, we found that PTEN protein levels are higher in SVF cells after several weeks in culture, connecting cellular age and adipogenic potential, which changes during long term culture. A recent study of tissue specific gene expression in mice during aging by Schaum *et al.* (31) showed a positive correlation of *PTEN* with age in subcutaneous fat depots, while most other tissues (including brown adipose tissue, but not mesenteric adipose tissue) showed a negative correlation. These results indicate a relevance of PTEN in adipose tissue aging, not only *in vitro* but also *in vivo*. *p16* and *p21* expression as well as SA-β-gal expression were reported to be higher in SVF cells from older donors (32). To test whether there is a direct effect of PTEN on cellular senescence, we compared *p16* and *p21* expression with and without PTEN knockdown and found a reduction in knockdown cells. We observed less SA-β-gal positive cells in SVF cells with CRISPR mediated PTEN downregulation. These results provide evidence for a connection between PTEN expression and cellular senescence. In contrast to pathway activation through PTEN downregulation, PI3K inhibition with alpelisib induced senescence in PTEN haploinsufficient lipoma cells (9) and PTEN overexpression was shown to induce G1 arrest in cancer cells mediated through AKT inhibition (33). We found *Cellular Senescence* to be the most significantly enriched KEGG-pathway in RNA sequencing of PTEN knockdown *vs*. control SVF cells, with senescence related genes like *CDKN2B* (34) and *HIPK2* (35) downregulated. A relation between PI3K/AKT pathway and aging was also reported in other stem cell types: mTOR complex 1 (mTORC1) activity in intestinal stem cells declines with aging (36). Age related upregulation of the upstream antagonist PTEN might be responsible for this decline in downstream PI3K signaling pathway activity and could also account for the age related decline in MSCs proliferation rate (32). On the other hand, there is strong evidence that inhibition of the insulin signaling pathway with a special focus on mTORC1 increases longevity. This makes sense in the context of insulin induced metabolic activity and increased reactive oxygen species (ROS) production (37). Some authors suggest an overproliferation and exhaustion of adipose progenitors in conditions of nutrient abundance associated with telomere shortening (38). Interestingly, Schumacher *et al*. found similarities in differential gene expression between mouse models of delayed and premature aging compared to wild-type mice, with downregulation of IGF-1 related pathways as a common feature (39). Varying PTEN expression might be a cellular mechanism to maintain a balance between senescence and overproliferation, ensuring normal adipose tissue homeostasis. In disease states PTEN downregulation leads to excessive adipose tissue growth and distribution abnormalities, while PTEN upregulation might contribute to senescence and dysfunctional adipose tissue in older individuals.

Experimental procedures

4.1 Cell culture and adipocyte differentiation

We used cells of the stromal vascular fraction isolated from visceral adipose tissue of healthy donors, resected during bariatric surgery as well as PTEN-haploinsufficient lipoma cells (LipPD1) from a pediatric PHTS patient (13) (Leipzig University ethical approval: no. 425-12-171220). All adipose tissue and lipoma tissue donors gave written informed consent to participate in the study. Isolation and culture methods were described previously (16, 40). Supplementary Table S4 contains a list of the primary cell cultures used.

For differentiation 15,000 cells/96-well or 120,000/12-well were plated in culture medium. Medium was changed to differentiation medium 24 h later (day 0) (DMEM/F12 containing 8 mg/ml D-biotin, 10 mg/ml D-pantothenic acid, 2 µM rosiglitazone, 25 nM dexamethasone, 0.5 mM methylisobuthylxantine, 0.1 µM cortisol, 0.01 mg/ml apotransferrin, 0.2 nM triiodotyronin, and 20 nM human insulin (41) and cells were kept in differentiation medium for 4, 8 or 12 days.

A modified method according to Klingelhutz *et al.* (23) was used for scaffold-free 3D cultures of SVF cells. After transfection 10,000 cells per well were seeded into low attachment 96-well microplates (PS, U-bottom, clear, cellstar®, cell-repellent surface, Greiner Bio-One) in 100 µl culture medium. After one day medium was changed to differentiation medium and spheroids were kept in differentiation medium for 12 days. Half of the medium was replaced every second day. Microscope images were taken daily using the EVOS FL Auto 2 Cell Imaging System (Invitrogen; Thermo Fisher Scientifc). Image analysis to determine the spheroid size was performed using ImageJ (42).

4.2 PTEN siRNA transfection

One day prior to transfection, cells were plated at a density of about 1,300 cells/cm² to ensure optimal growth. For transfection we used the Neon Transfection System 100 µl Kit (Invitrogen; Thermo Fisher Scientific, Inc.). Cells were harvested via trypsination and washed with DPBS. Either control siRNA (Silencer™ Negative Control No. 1 siRNA, Ambion, Thermo Fisher Scientific, Inc.) or a combination of *PTEN* siRNA (s325 and s326, both Ambion, Thermo Fisher Scientific, Inc.) was added to the cell pellets (final concentration of 10 nM in culture medium after transfection). Pellets were resuspended in 100 µl R-buffer for transfection and electroporated in Neon 100 µl tips at 1,300 V, 2 pulses, 20 ms. After electroporation cells were transferred to prewarmed culture medium and distributed to multiwell tissue culture plates for functional assays.

4.3 CRISPR/Cas *PTEN* knockout

For stable knockout of *PTEN* in SVF cells, we used the CRISPR/Cas9 genome editing technique in a reverse transfection of guideRNA/Cas9 nickase ribonucleoproteins (RNPs). Cas9 nickase was chosen to avoid off-target effects. If not otherwise stated, reagents were purchased from Integrated DNA Technologies (Alt-R CRISPR-Cas9 system). Transfections were performed according to the manufacturers' protocol with a combination of two different crRNA:tracrRNA guides and Alt-R S.p. Cas9 D10A Nickase 3 NLS (# 1078729). We tested combinations of four different crRNAs (Supplementary Table S5) for their editing efficiency via T7EI assay (Alt-R Genome Editing Detection Kit, # 1075931). For further assays we used the most efficient guide combination (#3 and #4). RNPs of Cas9 nickase and Alt-R CRISPR-Cas9 Negative Control crRNA #1 (#1072544) were used for controls.10,000 SVF cells per well were transfected in a 48-well format with a final concentration of 10 nM crRNA:tracrRNA:Cas9 nickase RNPs. We used a total volume of 300 µl per well with 2.4 µl Lipofectamin RNAiMAX (Thermo Fisher Scientific, #13778075). Efficiency was determined 2 days post transfection via T7EI assay.

4.4 Lipid staining

For lipid staining cells were fixed in 4% PFA and washed with DPBS. Afterwards cells were co-stained with the fluorescent dyes Nile Red (0.5 µg/ml, Sigma) and Hoechst 33342 (1 µg/ml, Sigma) for 5 min in DPBS. Microscope images were taken with the EVOS FL Auto 2 Cell Imaging System (Invitrogen; Thermo Fisher Scientific) and cell counting was performed with the Celleste Image Analysis Software (Thermo Fisher Scientific).

4.5 Proliferation assay

For proliferation assays cells were seeded at a density of 2,000 cells/well on 96-well plates. Growth medium was replaced every 72 h. Cells were fixed at day 1 and day 7 after transfection and kept in DPBS at 4 °C after fixation. Hoechst 33342 (Sigma) was used to stain nuclei for 5 min at a concentration of 1 µg/ml in DPBS. Hoechst fluorescence was detected at 455 nm and compared for day 1 and day 7.

4.6 Western blot analysis

For Western blot analysis transfected cells were seeded at a density of 10,000 cells/cm² in culture medium. Cell culture medium was replaced by serum free medium one day after transfection and cells were harvested on the next day. For Western blot analysis of long term cultures, cells were trypsinized during normal culture and 100,000 cells were frozen as a pellet. Proteins were extracted and immunoblotting was performed as described elsewhere (16). We used 10 µg protein per lane and incubated with primary antibodies

(Cell Signaling Technology, CST) and secondary antibodies (Dako; Agilent Technologies) according to Supplementary Table S6. α-Tubulin was used as loading control. Densitometric analysis was performed using ImageJ (42) and images of exposed films and their analysis are provided in the supplement Figure S2 (PTEN KD), Figure S3 (PTEN CR) and Figure S4 (long term culture).

4.7 Immunofluorescence staining

For Ki-67 immunofluorescence staining transfected cells were seeded at a density of 2,000 cells/well on 96-well plates and fixed with 4 % PFA after 24 h. Cells were permeabilized and blocked in IF-buffer (DPBS + 5 % BSA + 0.3 % Tween20) for 1 h at room temperature (RT) and stained with Ki-67 primary antibody over night at 4 °C (Supplementary Table S5). Cells were washed three times 5 min with IF-buffer and incubated with secondary Alexa Fluor 488 antibody (Supplementary Table S5) 2 h at RT in the dark. Afterwards cells were washed one time with IF-buffer, then incubated 5 min with 1 µg/ml Hoechst 33342 in DPBS and washed one time with DPBS. Microscope images were taken in DPBS using the EVOS FL Auto 2 Cell Imaging System (Invitrogen; Thermo Fisher Scientific) and cell counting was performed with the Celleste Image Analysis Software (Thermo Fisher Scientific).

4.8 Reverse transcription quantitative PCR (RT-qPCR)

We plated 6,000 cells/cm² for RT-qPCR of undifferentiated cells or 45,000 cells/cm² for differentiated cells. RNA extraction, reverse transcription and qPCR were performed as previously described (40). Supplementary Table S7 contains a list of primers used for qPCR assays. Results were normalized to the housekeepers *hypoxanthine phosphoribosyltransferase* (*HPRT*) and *TATA box binding protein* (*TBP*). We performed probe based assays using the Takyon™ Low Rox Probe MasterMix dTTP Blue (Eurogentec) or SYBR green assays using the Takyon™ Low Rox SYBR® MasterMix dTTP Blue (Eurogentec).

4.9 RNA-Sequencing

After PTEN knockdown we plated 6,000 cells/cm² in culture medium. Medium was replaced by serum free medium 1 day after transfection and cells were harvested 24 h afterwards. RNA was extracted as for RT-qPCRs. 100 ng of total RNA was used for library synthesis with the NEBNext Ultra II Directional RNA Library Preparation kit (New Endland Biolabs) according to the protocol of the manufacturer. The barcoded libraries were purified and quantified using the Library Quantification Kit - Illumina/Universal (KAPA Biosystems) on a TaqMan 7500 RealTime PCR System. A pool of up to 10 libraries was used for cluster generation at a concentration of 10 nM. Sequencing of 2x150 bp was

performed with a NextSeq 550 sequencer (Illumina) at the sequencing core facility of the Faculty of Medicine (Leipzig University) according to the instructions of the manufacturer.

4.9.1 Read Preprocessing and Mapping

Sequencing reads from 18 fastq files (triplicates of PTEN KD and controls from 3 donors) were mapped to the human reference genome (hg38 downloaded from UCSC/Ensembl (43)). Paired-end RNA-seq data were processed within the Galaxy platform (44). The raw sequencing reads (in fastq-format) were loaded to Galaxy instance and quality was inspected with fastqc (45). One sample (PTEN KD and the respective control) had to be removed from further analysis due to low quality. Reads were trimmed with TrimGalore! (46) and sufficient quality was ensured by a second quality check with fastqc. Subsequently, the reads were mapped to the human genome (hg38) with segemehl (47) and annotated with gencode.v29.

4.9.2 Differential Gene Expression and Gene Set Enrichment

For differential gene expression analysis with DESeq2 (48) only genes with at least ten mapped reads in at least half of the were kept samples reducing the analysis from 58,721 to 32,660 genes. After inspection of *PTEN* expression levels in all samples, we decided to exclude controls with only moderate *PTEN* expression levels to ensure clear distinguishability between high *PTEN* expression levels and *PTEN* knockdown. Thus controls 5, 11, and 15 were excluded from further analyses (Figure S5A). Afterwards, we ran DESeq2 to identify differentially expressed genes. A principle component analysis identified the different donors are the main source of variance, thus we corrected for the donor (batch) effect (Figure S5B), leading to better clustering of PTEN KD *vs*. control. We applied LFC shrinkage to reduce effect sizes of overall low expressed genes (shrinkage estimator ashr) (49).
Gene Set enrichment analysis was performed in STRING (string-db.org) (25). As input the 1379 significantly differentially expressed genes were used. The results were visualized using R custom scripts and the KEGG pathway visualization package pathview (50).

4.10 Statistical analysis

Means of at least three independent experiments were statistically analyzed using GraphPad Prism 6 software (GraphPad Software Inc.). For comparison of control and conditions of PTEN downregulation (PTEN KD or PTEN CR), means of independent experiments were compared via paired Student's t-test (comparison of each control transfection with the respective PTEN siRNA/PTEN CRISPR transfection). For multiple comparisons we used one- or two-way analysis of variance (ANOVA) followed by a post

hoc Tukey's multiple comparisons test (one-way ANOVA) or Dunnett's multiple comparisons test (two-way ANOVA). To determine the significance of fold changes, we used one-sample t-tests of the log fold change and compared to the hypothetical value 0 (51). Results were indicated as mean ± standard error of means (SEM).

Data availability statement

Gene lists and other supporting information are available at http://www.bioinf.uni-leipzig.de/publications/supplements/20-008.

Acknowledgments

We thank Prof. Dr. Arne Dietrich for giving us access to and all donors for providing adipose tissue samples. We thank Sandy Richter and Anja Barnikol-Oettler for the technical support in the laboratory.

Authors' contributions

AG, WK and ASK designed the study. ASK, AG, MN and JL performed the experimental work. SK performed the analysis and presentation of RNA-sequencing results. DLD and JB provided their RNA-sequencing results. ASK prepared the manuscript draft. All authors reviewed and edited the manuscript. Project administration, supervision and funding acquisition: AG, WK, MP, PFS and PK.

Funding and additional information

The project was supported by the German Research Foundation (209933838 - SFB 1052/Deutsche Forschungsgemeinschaft) and Mitteldeutsche Kinderkrebsforschung Stiftung für Forschung und Heilung. DLD is funded through "Clinician Scientist Program, Medizinische Fakultät der Universität Leipzig." PFS is also affiliated with the Institute of Theoretical Chemistry of the University of Vienna, Austria, the National University of Colombia, and the Santa Fe Institute. We acknowledge support from Leipzig University for Open Access Publishing.

Conflict of Interest

The authors declare no conflict of interest.

References

1. Kirkland, J. L., Tchkonia, T., Pirtskhalava, T., Han, J., and Karagiannides, I. (2002) Adipogenesis and aging: Does aging make fat go MAD? *Experimental Gerontology* **37**, 757–767 10.1016/S0531-5565(02)00014-1
2. Tchkonia, T., Morbeck, D. E., Zglinicki, T. von, van Deursen, J., Lustgarten, J., Scrable, H., Khosla, S., Jensen, M. D., and Kirkland, J. L. (2010) Fat tissue, aging, and cellular senescence. *Aging cell* **9**, 667–684 10.1111/j.1474-9726.2010.00608.x PMID 20701600
3. Yki-Jarvinen, H., Kiviluoto, T., and Nikkila, E. A. (1986) Insulin binding and action in adipocytes in vitro in relation to insulin action in vivo in young and middle-aged subjects. *Acta endocrinologica* **113**, 88–92 10.1530/acta.0.1130088 PMID 3532658
4. Cartwright, M. J., Tchkonia, T., and Kirkland, J. L. (2007) Aging in adipocytes: Potential impact of inherent, depot-specific mechanisms. *Experimental Gerontology* **42**, 463–471 10.1016/j.exger.2007.03.003 PMID 17507194
5. Cignarelli, A., Genchi, V. A., Perrini, S., Natalicchio, A., Laviola, L., and Giorgino, F. (2019) Insulin and Insulin Receptors in Adipose Tissue Development. *International journal of molecular sciences* **20** 10.3390/ijms20030759 PMID 30754657
6. Hauner, H., Entenmann, G., Wabitsch, M., Gaillard, D., Ailhaud, G., Negrel, R., and Pfeiffer, E. F. (1989) Promoting effect of glucocorticoids on the differentiation of human adipocyte precursor cells cultured in a chemically defined medium. *The Journal of clinical investigation* **84**, 1663–1670 10.1172/JCI114345 PMID 2681273
7. Wabitsch, M., Brenner, R. E., Melzner, I., Braun, M., Möller, P., Heinze, E., Debatin, K. M., and Hauner, H. (2001) Characterization of a human preadipocyte cell strain with high capacity for adipose differentiation. *International journal of obesity and related metabolic disorders : journal of the International Association for the Study of Obesity* **25**, 8–15 10.1038/sj.ijo.0801520 PMID 11244452
8. Bell, A., Grunder, L., and Sorisky, A. (2000) Rapamycin inhibits human adipocyte differentiation in primary culture. *Obesity research* **8**, 249–254 10.1038/oby.2000.29 PMID 10832768
9. Kirstein, A. S., Augustin, A., Penke, M., Cea, M., Körner, A., Kiess, W., and Garten, A. (2019) The Novel Phosphatidylinositol-3-Kinase (PI3K) Inhibitor Alpelisib Effectively Inhibits Growth of PTEN-Haploinsufficient Lipoma Cells. *Cancers* **11** 10.3390/cancers11101586 PMID 31627436
10. Blüher, M., Kahn, B. B., and Kahn, C. R. (2003) Extended longevity in mice lacking the insulin receptor in adipose tissue. *Science (New York, N.Y.)* **299**, 572–574 10.1126/science.1078223 PMID 12543978
11. Bartke, A. (2008) Impact of reduced insulin-like growth factor-1/insulin signaling on aging in mammals: Novel findings. *Aging cell* **7**, 285–290 10.1111/j.1474-9726.2008.00387.x PMID 18346217
12. Katic, M., Kennedy, A. R., Leykin, I., Norris, A., McGettrick, A., Gesta, S., Russell, S. J., Bluher, M., Maratos-Flier, E., and Kahn, C. R. (2007) Mitochondrial gene expression and increased oxidative metabolism: Role in increased lifespan of fat-specific insulin receptor knock-out mice. *Aging cell* **6**, 827–839 10.1111/j.1474-9726.2007.00346.x PMID 18001293

13. Kässner, F., Kirstein, A., Händel, N., Schmid, G. L., Landgraf, K., Berthold, A., Tannert, A., Schaefer, M., Wabitsch, M., Kiess, W., Körner, A., and Garten, A. (2020) A new human adipocyte model with PTEN haploinsufficiency. *Adipocyte* **9**, 290–301 10.1080/21623945.2020.1785083 PMID 32579864
14. Saxton, R. A., and Sabatini, D. M. (2017) mTOR Signaling in Growth, Metabolism, and Disease. *Cell* **168**, 960–976 10.1016/j.cell.2017.02.004 PMID 28283069
15. Simpson, L., and Parsons, R. (2001) PTEN: Life as a tumor suppressor. *Experimental cell research* **264**, 29–41 10.1006/excr.2000.5130 PMID 11237521
16. Schmid, G. L., Kässner, F., Uhlig, H. H., Körner, A., Kratzsch, J., Händel, N., Zepp, F.-P., Kowalzik, F., Laner, A., Starke, S., Wilhelm, F. K., Schuster, S., Viehweger, A., Hirsch, W., Kiess, W., and Garten, A. (2014) Sirolimus treatment of severe PTEN hamartoma tumor syndrome: Case report and in vitro studies. *Pediatric research* **75**, 527–534 10.1038/pr.2013.246 PMID 24366516
17. Huang, W., Queen, N. J., McMurphy, T. B., Ali, S., and Cao, L. (2019) Adipose PTEN regulates adult adipose tissue homeostasis and redistribution via a PTEN-leptin-sympathetic loop. *Molecular metabolism* **30**, 48–60 10.1016/j.molmet.2019.09.008 PMID 31767180
18. Sanchez-Gurmaches, J., Hung, C.-M., Sparks, C. A., Tang, Y., Li, H., and Guertin, D. A. (2012) PTEN loss in the Myf5 lineage redistributes body fat and reveals subsets of white adipocytes that arise from Myf5 precursors. *Cell metabolism* **16**, 348–362 10.1016/j.cmet.2012.08.003 PMID 22940198
19. Filtz, E. A., Emery, A., Lu, H., Forster, C. L., Karasch, C., and Hallstrom, T. C. (2015) Rb1 and Pten Co-Deletion in Osteoblast Precursor Cells Causes Rapid Lipoma Formation in Mice. *PloS one* **10**, e0136729 10.1371/journal.pone.0136729 PMID 26317218
20. Hsieh, S.-C., Chen, N.-T., and Lo, S. H. (2009) Conditional loss of PTEN leads to skeletal abnormalities and lipoma formation. *Molecular carcinogenesis* **48**, 545–552 10.1002/mc.20491 PMID 18973188
21. Chu, C.-Y., Chen, C.-F., Rajendran, R. S., Shen, C.-N., Chen, T.-H., Yen, C.-C., Chuang, C.-K., Lin, D.-S., and Hsiao, C.-D. (2012) Overexpression of Akt1 Enhances Adipogenesis and Leads to Lipoma Formation in Zebrafish. *PLOS ONE* **7**, e36474 10.1371/journal.pone.0036474
22. Fagerberg, L., Hallström, B. M., Oksvold, P., Kampf, C., Djureinovic, D., Odeberg, J., Habuka, M., Tahmasebpoor, S., Danielsson, A., Edlund, K., Asplund, A., Sjöstedt, E., Lundberg, E., Szigyarto, C. A.-K., Skogs, M., Takanen, J. O., Berling, H., Tegel, H., Mulder, J., Nilsson, P., Schwenk, J. M., Lindskog, C., Danielsson, F., Mardinoglu, A., Sivertsson, A., Feilitzen, K. von, Forsberg, M., Zwahlen, M., Olsson, I., Navani, S., Huss, M., Nielsen, J., Ponten, F., and Uhlén, M. (2014) Analysis of the human tissue-specific expression by genome-wide integration of transcriptomics and antibody-based proteomics. *Molecular & cellular proteomics : MCP* **13**, 397–406 10.1074/mcp.M113.035600 PMID 24309898
23. Klingelhutz, A. J., Gourronc, F. A., Chaly, A., Wadkins, D. A., Burand, A. J., Markan, K. R., Idiga, S. O., Wu, M., Potthoff, M. J., and Ankrum, J. A. (2018) Scaffold-free generation of uniform adipose spheroids for metabolism research and drug discovery. *Scientific Reports* **8**, 523 10.1038/s41598-017-19024-z

24. Yoshino, J., Mills, K. F., Yoon, M. J., and Imai, S.-i. (2011) Nicotinamide mononucleotide, a key NAD(+) intermediate, treats the pathophysiology of diet- and age-induced diabetes in mice. *Cell metabolism* **14**, 528–536 10.1016/j.cmet.2011.08.014 PMID 21982712
25. Szklarczyk, D., Gable, A. L., Lyon, D., Junge, A., Wyder, S., Huerta-Cepas, J., Simonovic, M., Doncheva, N. T., Morris, J. H., Bork, P., Jensen, L. J., and Mering, C. von (2019) STRING v11: protein-protein association networks with increased coverage, supporting functional discovery in genome-wide experimental datasets. *Nucleic acids research* **47**, D607-D613 10.1093/nar/gky1131 PMID 30476243
26. Le Duc, D., Lin, C.-C., Popkova, Y., Yang, Z., Akhil, V., Çakir, M. V., Grunewald, S., Simon, J.-C., Dietz, A., Dannenberger, D., Garten, A., Lemke, J. R., Schiller, J., Blüher, M., Nono Nankam, P. A., Rolle-Kampczyk, U., Bergen, M. von, Kelso, J., and Schöneberg, T. (2020) Reduced lipolysis in lipoma phenocopies lipid accumulation in obesity. *International journal of obesity (2005)* 10.1038/s41366-020-00716-y PMID 33235355
27. Breitfeld, J., Kehr, S., Müller, L., Stadler, P. F., Böttcher, Y., Blüher, M., Stumvoll, M., and Kovacs, P. (2020) Developmentally Driven Changes in Adipogenesis in Different Fat Depots Are Related to Obesity. *Frontiers in Endocrinology* **11**, 138 10.3389/fendo.2020.00138 PMID 32273869
28. Hirsch, J., and Batchelor, B. (1976) Adipose tissue cellularity in human obesity. *Clinics in Endocrinology and Metabolism* **5**, 299–311 10.1016/S0300-595X(76)80023-0
29. García, Z., Kumar, A., Marqués, M., Cortés, I., and Carrera, A. C. (2006) Phosphoinositide 3-kinase controls early and late events in mammalian cell division. *The EMBO journal* **25**, 655–661 10.1038/sj.emboj.7600967 PMID 16437156
30. Pal, A., Barber, T. M., van de Bunt, M., Rudge, S. A., Zhang, Q., Lachlan, K. L., Cooper, N. S., Linden, H., Levy, J. C., Wakelam, M. J. O., Walker, L., Karpe, F., and Gloyn, A. L. (2012) PTEN mutations as a cause of constitutive insulin sensitivity and obesity. *The New England journal of medicine* **367**, 1002–1011 10.1056/NEJMoa1113966 PMID 22970944
31. Schaum, N., Lehallier, B., Hahn, O., Pálovics, R., Hosseinzadeh, S., Lee, S. E., Sit, R., Lee, D. P., Losada, P. M., Zardeneta, M. E., Fehlmann, T., Webber, J. T., McGeever, A., Calcuttawala, K., Zhang, H., Berdnik, D., Mathur, V., Tan, W., Zee, A., Tan, M., Pisco, A. O., Karkanias, J., Neff, N. F., Keller, A., Darmanis, S., Quake, S. R., and Wyss-Coray, T. (2020) Ageing hallmarks exhibit organ-specific temporal signatures. *Nature* **153**, 1194 10.1038/s41586-020-2499-y
32. Choudhery, M. S., Badowski, M., Muise, A., Pierce, J., and Harris, D. T. (2014) Donor age negatively impacts adipose tissue-derived mesenchymal stem cell expansion and differentiation. *Journal of translational medicine* **12**, 8 10.1186/1479-5876-12-8 PMID 24397850
33. Ramaswamy, S., Nakamura, N., Vazquez, F., Batt, D. B., Perera, S., Roberts, T. M., and Sellers, W. R. (1999) Regulation of G1 progression by the PTEN tumor suppressor protein is linked to inhibition of the phosphatidylinositol 3-kinase/Akt pathway. *PNAS* **96**, 2110–2115 10.1073/pnas.96.5.2110
34. Tu, Q., Hao, J., Zhou, X., Yan, L., Dai, H., Sun, B., Yang, D., An, S., Lv, L., Jiao, B., Chen, C., Lai, R., Shi, P., and Zhao, X. (2018) CDKN2B deletion is essential for pancreatic cancer development instead

of unmeaningful co-deletion due to juxtaposition to CDKN2A. *Oncogene* **37**, 128–138 10.1038/onc.2017.316 PMID 28892048

35. Feng, Y., Zhou, L., Sun, X., and Li, Q. (2017) Homeodomain-interacting protein kinase 2 (HIPK2): a promising target for anti-cancer therapies. *Oncotarget* **8**, 20452–20461 10.18632/oncotarget.14723 PMID 28107201
36. Igarashi, M., Miura, M., Williams, E., Jaksch, F., Kadowaki, T., Yamauchi, T., and Guarente, L. (2019) NAD+ supplementation rejuvenates aged gut adult stem cells. *Aging cell* **18**, e12935 10.1111/acel.12935 PMID 30917412
37. Berniakovich, I., Trinei, M., Stendardo, M., Migliaccio, E., Minucci, S., Bernardi, P., Pelicci, P. G., and Giorgio, M. (2008) p66Shc-generated oxidative signal promotes fat accumulation. *The Journal of biological chemistry* **283**, 34283–34293
38. Eckel-Mahan, K., Ribas Latre, A., and Kolonin, M. G. (2020) Adipose Stromal Cell Expansion and Exhaustion: Mechanisms and Consequences. *Cells* **9** 10.3390/cells9040863 PMID 32252348
39. Schumacher, B., van der Pluijm, I., Moorhouse, M. J., Kosteas, T., Robinson, A. R., Suh, Y., Breit, T. M., van Steeg, H., Niedernhofer, L. J., van Ijcken, W., Bartke, A., Spindler, S. R., Hoeijmakers, J. H. J., van der Horst, G. T. J., and Garinis, G. A. (2008) Delayed and accelerated aging share common longevity assurance mechanisms. *PLoS genetics* **4**, e1000161 10.1371/journal.pgen.1000161 PMID 18704162
40. Kässner, F., Sauer, T., Penke, M., Richter, S., Landgraf, K., Körner, A., Kiess, W., Händel, N., and Garten, A. (2018) Simvastatin induces apoptosis in PTEN-haploinsufficient lipoma cells. *International journal of molecular medicine* **41**, 3691–3698 10.3892/ijmm.2018.3568 PMID 29568880
41. Fischer-Posovszky, P., Newell, F. S., Wabitsch, M., and Tornqvist, H. E. (2008) Human SGBS cells - a unique tool for studies of human fat cell biology. *Obesity facts* **1**, 184–189 10.1159/000145784 PMID 20054179
42. Schneider, C. A., Rasband, W. S., and Eliceiri, K. W. (2012) NIH Image to ImageJ: 25 years of Image Analysis. *Nature methods* **9**, 671–675 PMID 22930834
43. (27.11.2020) *UCSC Genome Browser Home.* https://genome.ucsc.edu/index.html
44. Afgan, E., Baker, D., Batut, B., van den Beek, M., Bouvier, D., Cech, M., Chilton, J., Clements, D., Coraor, N., Grüning, B. A., Guerler, A., Hillman-Jackson, J., Hiltemann, S., Jalili, V., Rasche, H., Soranzo, N., Goecks, J., Taylor, J., Nekrutenko, A., and Blankenberg, D. (2018) The Galaxy platform for accessible, reproducible and collaborative biomedical analyses: 2018 update. *Nucleic acids research* **46**, W537-W544 10.1093/nar/gky379 PMID 29790989
45. Andrews, S. (2010) *Babraham Bioinformatics - FastQC A Quality Control tool for High Throughput Sequence Data.* https://www.bioinformatics.babraham.ac.uk/projects/fastqc/
46. Krueger, F. (2012) *Babraham Bioinformatics - Trim Galore!* http://www.bioinformatics.babraham.ac.uk/projects/trim_galore/
47. Hoffmann, S., Otto, C., Kurtz, S., Sharma, C. M., Khaitovich, P., Vogel, J., Stadler, P. F., and Hackermüller, J. (2009) Fast mapping of short sequences with mismatches, insertions and deletions

using index structures. *PLoS computational biology* **5**, e1000502 10.1371/journal.pcbi.1000502 PMID 19750212

48. Love, M. I., Huber, W., and Anders, S. (2014) Moderated estimation of fold change and dispersion for RNA-seq data with DESeq2. *Genome biology* **15**, 550 10.1186/s13059-014-0550-8 PMID 25516281
49. Stephens, M. (2017) False discovery rates: a new deal. *Biostatistics (Oxford, England)* **18**, 275–294 10.1093/biostatistics/kxw041 PMID 27756721
50. Luo, W., and Brouwer, C. (2013) Pathview: an R/Bioconductor package for pathway-based data integration and visualization. *Bioinformatics (Oxford, England)* **29**, 1830–1831 10.1093/bioinformatics/btt285 PMID 23740750
51. Tsai, C.-A., Chen, Y.-J., and Chen, J. J. (2003) Testing for differentially expressed genes with microarray data. *Nucleic acids research* **31**, e52 PMID 12711697

Figures

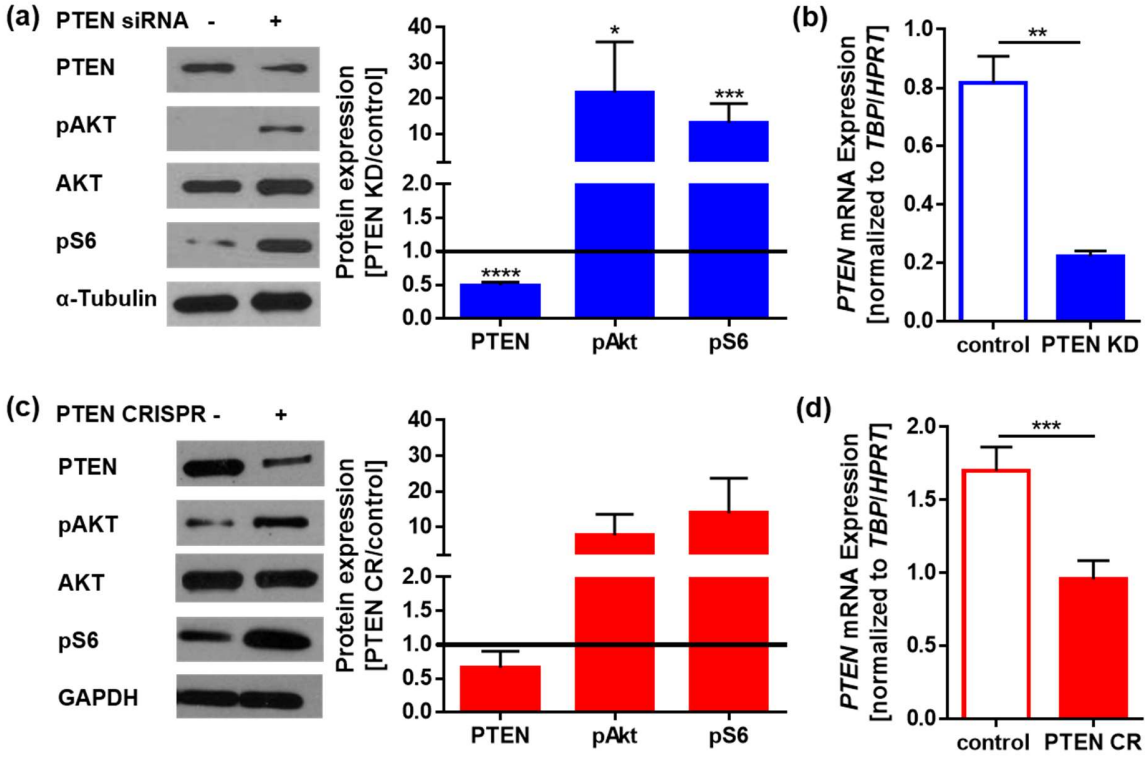

Figure 1: PTEN downregulation enhances PI3K signaling. (a) Western blots of control and PTEN siRNA (PTEN KD) transfected SVF cells: PTEN was reduced to 0.49 ± 0.05 fold (normalized to α-Tubulin, n=18, p<0.0001), phosphorylated AKT (pAKT (T308)) was elevated 22 ± 14 fold (normalized to total AKT, n=7, p=0.029) and ribosomal protein S6 phosphorylation (pS6 (Ser235/236)) was increased 13.03 ± 5.5 fold (normalized to α-Tubulin, n=11, p=0.0008). (b) *PTEN* mRNA expression in control and PTEN siRNA transfected SVF cells: *PTEN* was reduced to 0.33 ± 0.08 fold (normalized to means of *hypoxanthine phosphoribosyltransferase* (*HPRT*) and *TATA-box binding protein* (*TBP*) expression, n=4, p=0.0039). (c)

Western blots of control and PTEN CRISPR (PTEN CR) SVF cells: PTEN was reduced to 0.7 ± 0.3 fold (normalized to α-Tubulin, n=4, p=0.27), pAKT (T308) was increased 8 ± 6 fold (normalized to total AKT, n=4, p=0.24) and pS6 (Ser235/236) was increased 14 ± 10 fold (normalized to α-Tubulin, n=4, p=0.09). (d) *PTEN* mRNA expression in control and PTEN CR cells: *PTEN* was reduced to 0.56 ± 0.05 fold (p=0.0002) (normalized to *HPRT* and *TBP*, n=4, p=0.0002). p-values for (a) and (c) were determined via one-sample t-test of the log fold change, p-values for (b) and (d) were determined via paired t-test.

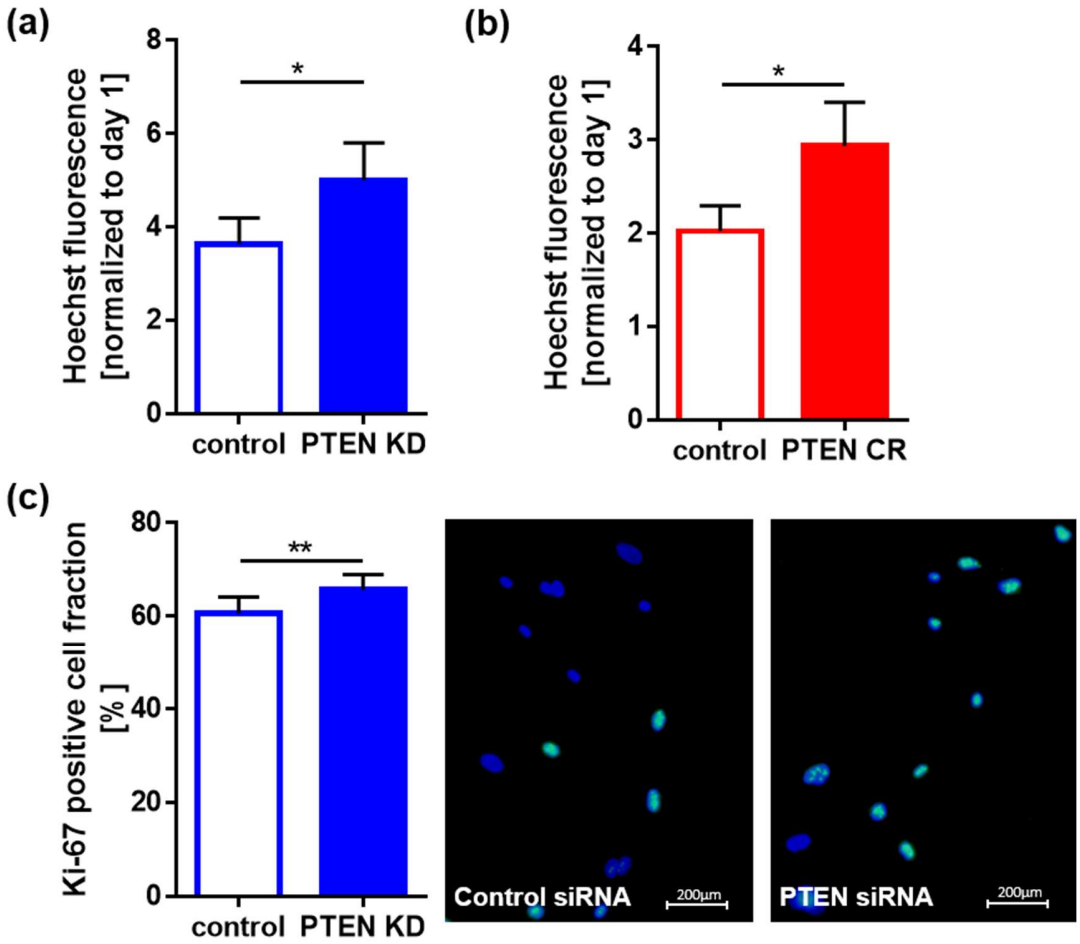

Figure 2: PTEN downregulation enhances proliferation. (a) Hoechst nuclei staining of control and PTEN KD cells 7 days after transfection: Proliferation in PTEN KD cells was increased 1.4 ± 0.2 fold (n=8, p=0.038). (b) Hoechst nuclei staining of control and PTEN CR cells 7 days after plating: Proliferation in PTEN CR cells was increased 1.5 ± 0.1 fold (n=5, p=0.039). (c) Ki-67 immunofluorescence staining in control and PTEN KD cells 1 day after transfection: PTEN KD cells show 1.09 ± 0.01 fold (n=3, p=0.0043) higher fraction of proliferation marker Ki-67 positive cells. p-values were determined via paired t-test.

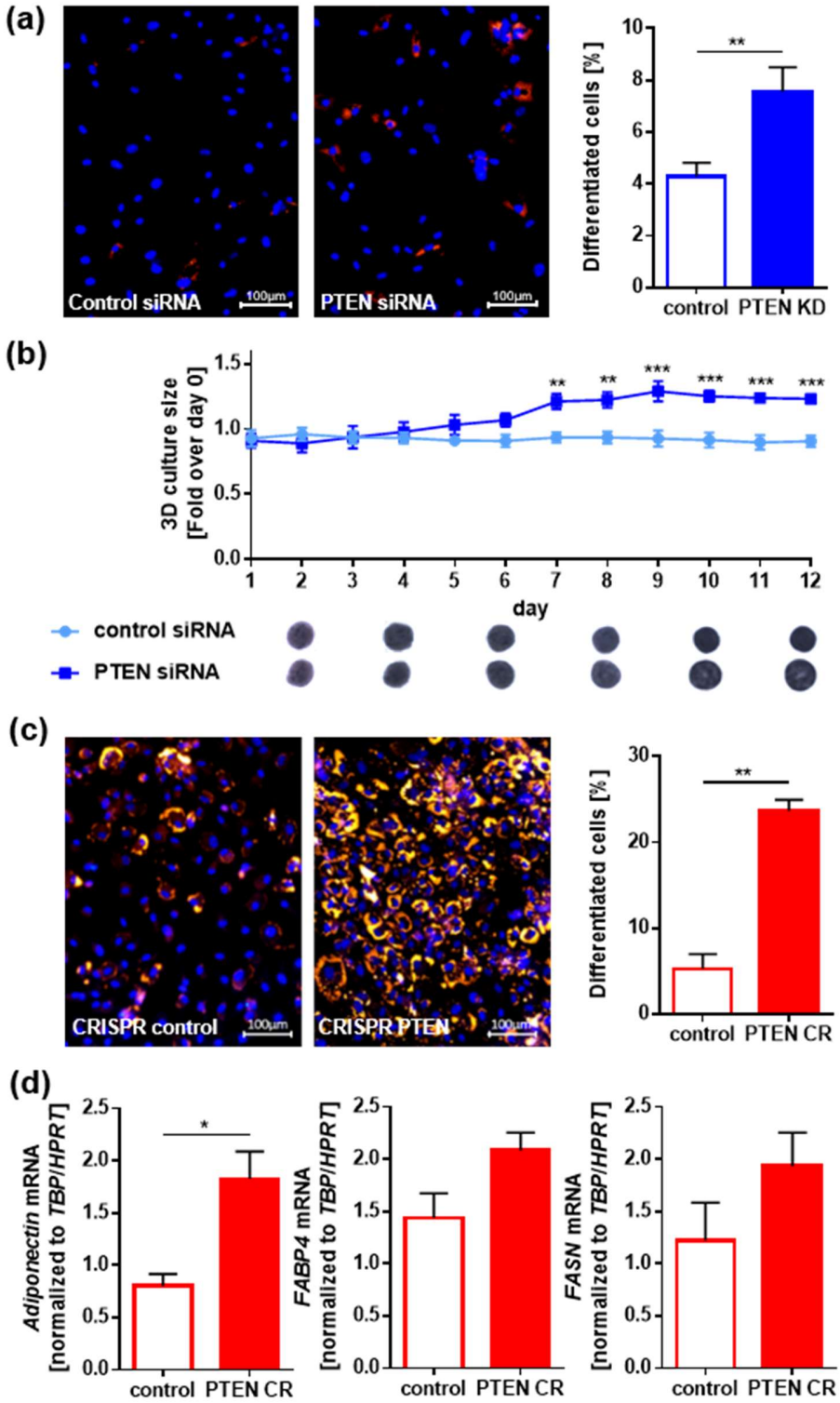

Figure 3: PTEN downregulation enhances adipogenesis. (a) Hoechst nuclei staining (blue) and Nile Red lipid staining (red) in high-passage SVF cells with or without PTEN KD after 8 days in adipogenic medium: The fraction of differentiated cells increased 1.77 ± 0.07 fold (n=5, p=0.0026) after PTEN knockdown. (b)

3D culture of control and PTEN KD SVF cells in adipogenic medium for 12 days: The size of control SVF cell spheroids remained constant over 12 days while it was increased 1.23 ± 0.03 fold (n=4, p<0.001) for PTEN KD spheroids (** p<0.01, *** p<0.001). (c) Hoechst nuclei staining (blue) and Nile Red lipid staining (red) in high-passage control or PTEN CR SVF cells after 8 days in adipogenic medium: The fraction of differentiated cells was increased 5.6 ± 1.9 fold (n=3, p=0.004) in CRISPR PTEN knockout cells compared to controls. (d) Expression of the adipocyte markers in control or PTEN CR SVF cells after 8 days in adipogenic medium: *adiponectin* expression was increased in PTEN CR cells 2.6 ± 0.6 fold (normalized to *HPRT* and *TBP*, n=6, p=0.016), *fatty acid synthase* (*FASN*) 2.1 ± 0.8 fold (normalized to *HPRT* and *TBP*, n=4, p=0.075) and *fatty acid binding protein 4* (*FABP4*) 1.9 ± 0.6 fold (normalized to *HPRT* and *TBP*, n=6, p=0.078) compared to controls. p-values were determined via paired t-test.

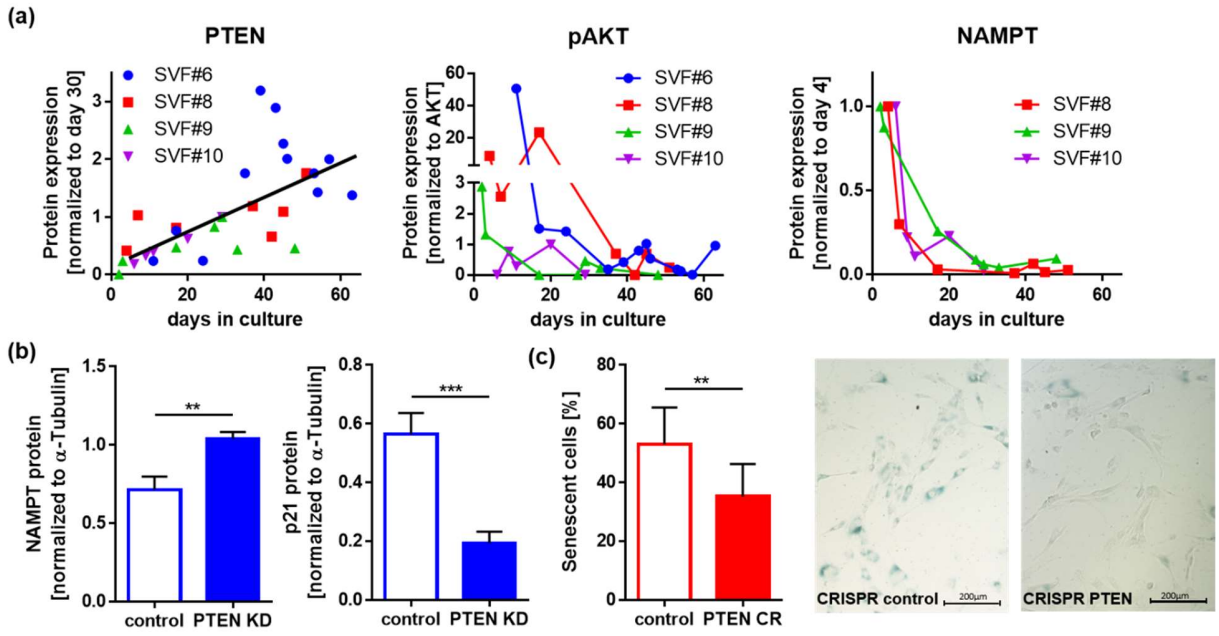

Figure 4: PTEN levels increase during cellular aging. (a) Western blots of primary SVF cells at different days in culture: PTEN levels increased during long term culture (normalized to α-Tubulin, p < 0.0001), while the ratio of pAKT (T308) to total AKT (p=0.1) and nicotinamide phosphoribosyltransferase (NAMPT, normalized to α-Tubulin, p=0.0004) decreased during long term culture. (b) Western blots of control and PTEN KD SVF cells: NAMPT protein increased 1.6 ± 0.2 fold (normalized to α-Tubulin, n=7, p=0.0029) while p21 protein decreased to 0.33 ± 0.07 fold (normalized to α-Tubulin, n=8, p=0.0004) in PTEN KD cells. (c) Senescence-associated β-galactosidase (SA-β-gal) assay of control and PTEN CR cells after long term culture: the fraction of SA-β-gal positive cells was 1.58 ± 0.12 fold (n=3, p=0.0098) increased in the controls. p-values for (a) were determined via linear regression and correlation analysis, p-values for (b) and (c) were determined via paired t-test.

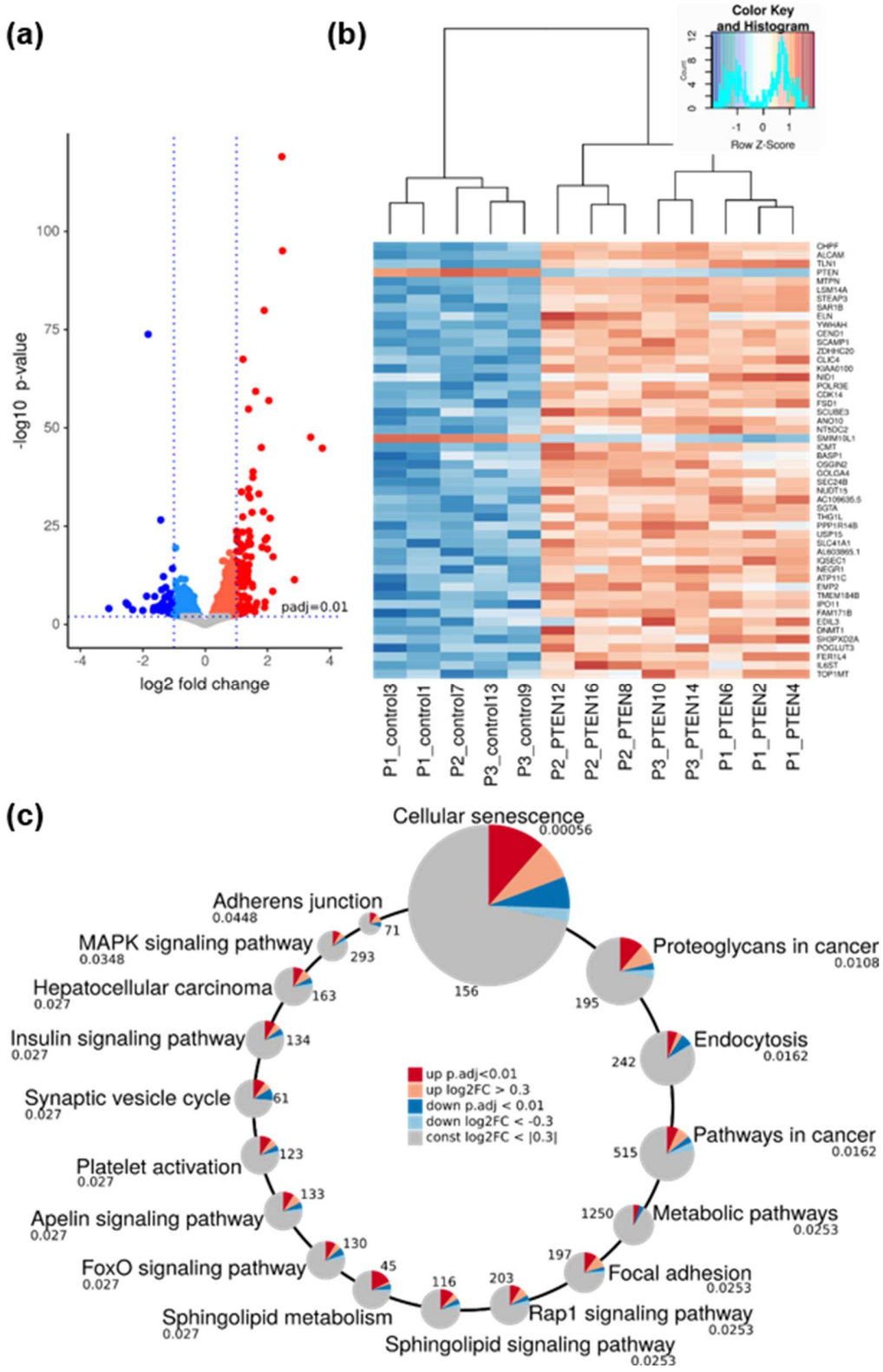

Figure 5: RNA Sequencing of PTEN knockdown and control SVF cells. (a) Volcano plot of differential gene expression in control *vs.* PTEN KD cells: we found 829 upregulated genes (red) and 550 downregulated genes (blue) (adjusted p<0.01). Of those 115 up- and 55 down- regulated genes had a

log2 fold change (log2FC) >1 or <-1, which means at least duplication or halving of mRNA transcripts. (b) Heatmap of differentially expressed genes in control *vs*. PTEN KD cells: among the 50 most significantly differentially expressed genes only *PTEN* and *SMIM10L1* were downregulated, while the majority of genes were upregulated. (c) Differentially expressed genes were significantly enriched (adjusted p<0.05) in 18 KEGG-pathways. The circles scale for adjusted p-values, which are given below the pathway name. Numbers next to the circles give the total number of genes assigned to the pathway in KEGG. Dark red and blue slices represent the fractions of significantly up and downregulated genes in the pathways. Light red and blue slices mark additional fractions, where the expression is altered by at least 20% (log2FC >|0.3|), although the expression change was not significant.

Supporting information figure legends

Complete supporting information is available at http://www.bioinf.uni-leipzig.de/publications/supplements/20-008.

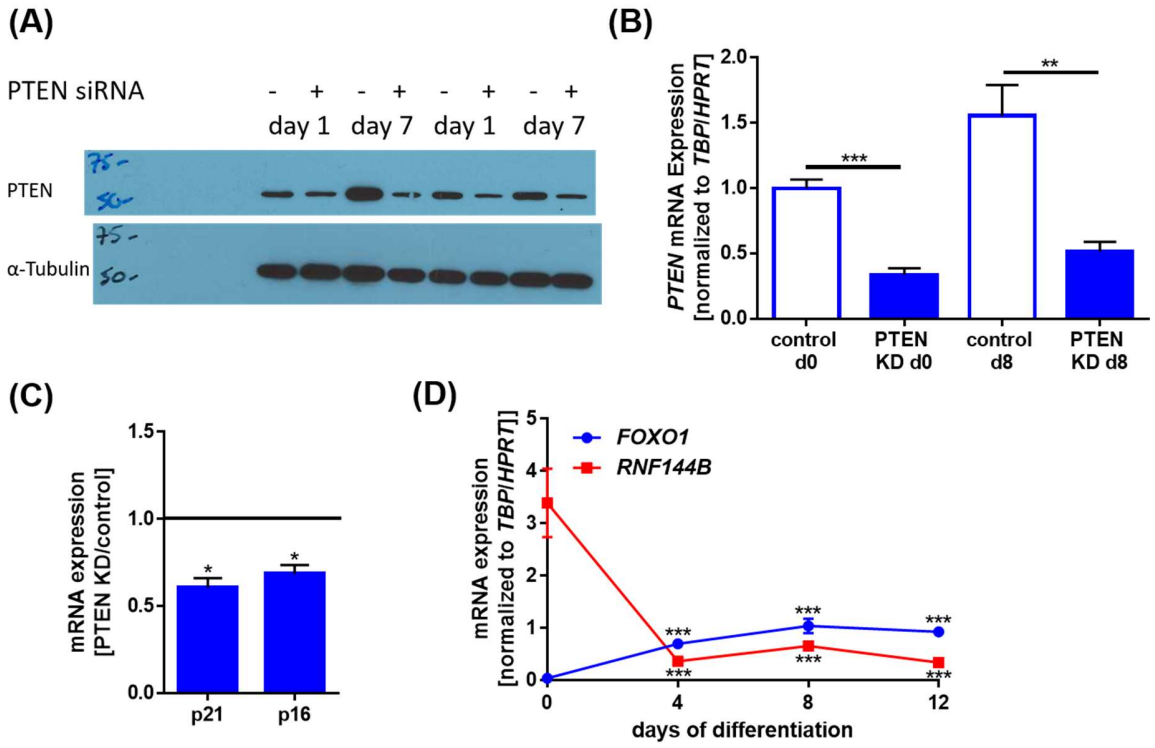

Figure S1: (A) Western blots of PTEN KD/control SVF cells: PTEN knockdown was stable for 7 days after siRNA transfection. (B) *PTEN* mRNA expression in PTEN KD/control SVF cells: *PTEN* was downregulated in PTEN KD cells upon induction of differentiation (d0) (one day after transfection) and after eight days of adipose differentiation (d8). (C) Senescence marker mRNA expression of PTEN KD/control SVF cells: on mRNA level we found a reduction of *p21* (to 0.6 ± 0.06 fold, n=3, p=0.031) and senescence marker *p16* (to 0.68 ± 0.05 fold, n=4, p=0.014). (D) Gene expression of *FOXO1* and *RNF144B* during adipogenesis: *FOXO1* was upregulated during adiocyte development while *RNF144B* was downregulated (n=4, *** p<0.001).

Figure S2: Western blots of PTEN KD/control SVF cells: exposed films and densitometric analyses of PTEN (normalized to α-Tubulin), pAKT (T308) (normalized to total AKT), pS6 (Ser235/236) (normalized to α-Tubulin), NAMPT(normalized to α-Tubulin) and p21 (normalized to α-Tubulin).

Figure S3: Western blots of PTEN CR/control SVF cells: exposed films and densitometric analyses of PTEN (normalized to α-Tubulin), pAKT (T308) (normalized to total AKT) and pS6 (Ser235/236) (normalized to α-Tubulin).

Figure S4: Western blots of four SVF cell long term cultures: exposed films and densitometric analyses of PTEN (normalized to α-Tubulin), pAKT (T308) (normalized to total AKT) and pS6 (Ser235/236) (normalized to α-Tubulin).

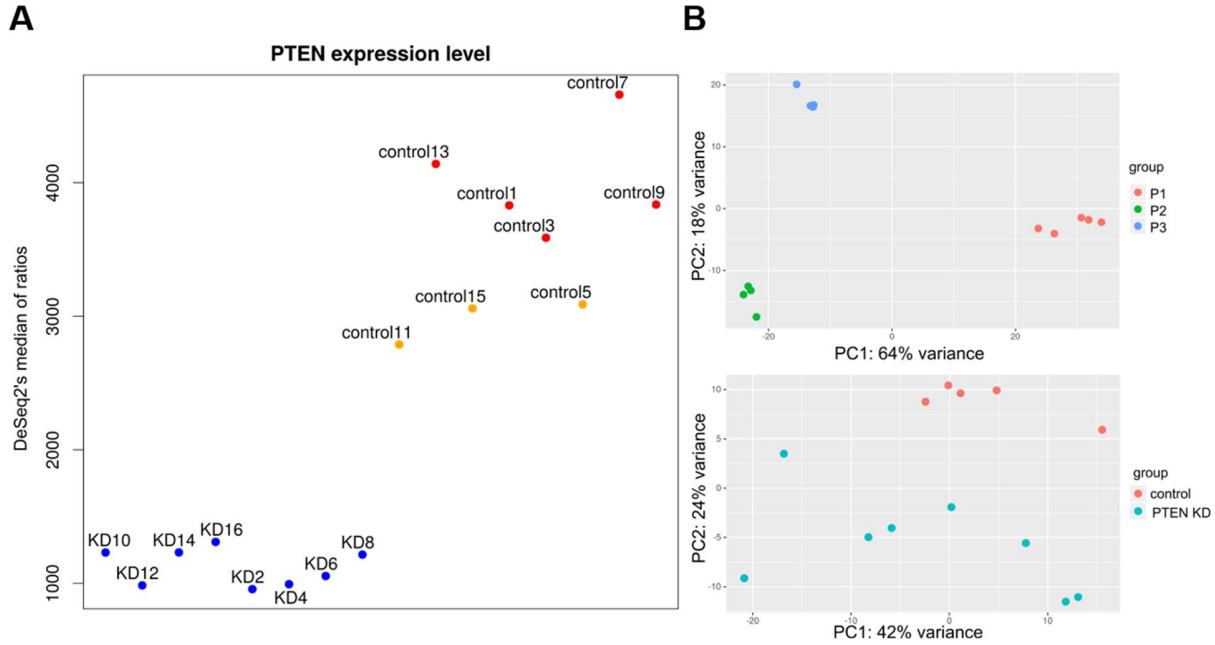

Figure S5: (A) Normalized read counts mapping to *PTEN* mRNA in the investigated samples. (B) PCA of samples clearly cluster according patients (upper panel), after removing the variance caused by the individual cell donors the second principal component (PC2) segregates the samples into control *vs*. PTEN (lower panel).